Particle migration induced by confinement of colloidal suspensions along the gravitational direction

J. J. Liétor-Santos and A. Fernández-Nieves
Group of Complex Fluids Physics, Department of Applied Physics, University of Almeria, Almeria 04120, Spain

M. Márquez
Interdisciplinary Network of Emerging Science and Technology (INEST) Group, Research Center, Phillip Morris USA, Richmond, Virginia 23234, USA; Harrington Department of Bioengineering, Arizona State University, Tempe, Arizona 85287, USA; and NIST Center for Theoretical and Computational Nanosciences, Gaithersburg, Maryland 20899, USA
(Received 14 May 2006; published 16 November 2006)

We confine charged spheres in cells with the smallest dimension along the direction of gravity $\hat{g}$. The particles are density mismatched with the surrounding medium and sediment along $\hat{g}$ with typical Péclet numbers of $\mathrm{Pe} \approx 10^{-3}$. After a certain time, we find that the number of particles N increases near both upper and lower plates until a characteristic time τ is reached; above this time N plateaus. We attribute the observed phenomenology to collective particle motions driven by gravity and mediated by hydrodynamic interactions; these could yield formation of swirls made of particles with correlated velocities that could eventually drive the particles towards the upper plate. The characteristic time for these migrations scales with plate-to-plate separation L_z as $\tau \sim L_z^{1.2}$, exactly as the characteristic decay time of velocity fluctuations in sedimentation processes [S. Y. Tee *et al.*, Phys. Rev. Lett. **89**, 054501 (2002)], despite that in these experiments the smallest cell dimension is perpendicular to $\hat{g}$ and $7 < \mathrm{Pe} < 50$. In the absence of gravitational field, the observed particle migrations disappear, emphasizing the key role played by gravity in these experiments.

DOI: 10.1103/PhysRevE.74.051404 PACS number(s): 82.70.Dd, 47.57.ef

I. INTRODUCTION

Colloidal suspensions consist of many interacting particles dispersed in a liquid. The interactions can have different origin; they can be mediated via the medium hydrodynamically, arise from dispersion forces, or be electrostatic in nature. The intrinsic many body character of these systems has motivated studies ranging from theoretical physics [1–3] to molecular biology [4–6] further promoting a strong connection between basic science and technology; paints [7] and food colloids [8] are examples of this interchange. In almost all cases, the colloidal suspension needs to be confined within bounding surfaces due to its intrinsic liquid properties.

In the case of charged colloidal suspensions, it has been theoretically predicted that confinement leads to an electrostatically driven adsorption of the particles onto the confining walls [9]. Intuitively, the system overall electrostatic energy is reduced if some particles in the bulk are pushed towards the suspension boundaries. The relevance of this effect depends on particle volume fraction ϕ, strength, and range of the interactions and may occur irrespective of the sign and magnitude of the confining walls' charge. In fact, this effect could lead to *charging* of neutral walls.

Body forces also affect the system equilibrium state and can cause particle accumulation in the boundaries. Gravity is perhaps the most common example, since density matched systems are the exception rather than the rule. Particles may then sediment or cream depending on the sign of the density mismatch $\Delta\rho$.

The influence of gravity on the settling or creaming of colloidal suspensions has been studied both from theoretical [10–12] and simulation [13,14] points of view revealing the existence of intriguing velocity fluctuations about the mean. These arise from unavoidable hydrodynamic interactions and induce the appearance of regions of particles with correlated velocities that behave as swirls reminding of convective fluxes, despite that Reynolds numbers are always low in these studies [15].

Recently, some experiments with hard spheres confined in containers whose larger dimension lies along the gravitational direction have revealed the existence of those swirls and have determined that their size scales with the particle volume fraction as $a\phi^{-1/3}$, with a the particle radius [16–19]. Moreover, it has been found that velocity fluctuations decay in time exponentially with a characteristic time that scales with the height of the container [18]. The reason for this decay could rest on the presence of boundaries inducing the spread of the sedimentation front, as argued in recent computer simulations [20]. In all these experiments Péclet numbers $\mathrm{Pe} = \frac{v_s a}{D}$, with v_s the mean sedimentation velocity and D the diffusion coefficient, are above 1.

In this work, we will focus in the case where the smallest container dimension is the one parallel to gravity (Fig. 1) and Péclet numbers are of order 10^{-3}. We present experimental measurements for charged hard spheres confined between two optically transparent plates surrounded by an almost density matched medium, and study the evolution in time of the number of particles near the lower and upper walls and in the bulk using optical microscopy. We find an expected increase in the number of particles in the plate favored either by sedimentation or creaming of the suspension, but an apparent surprising raise in the other plate too. The physics of this latter increase could rely on the electrostatically driven adsorption described above; however, we measure the particles' effective charge with the aid of electrophoresis and

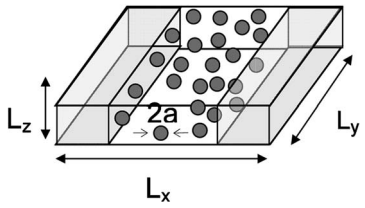

FIG. 1. Schematic of the experimental setup. The horizontal cell dimensions are $L_x \approx L_y \approx 2.5$ cm. L_z is changed in the experiments but is always the smallest dimension. Gravity points in the z direction along L_z.

estimate particle-particle interactions with the Derjaguin-Landau-Verwey-Overbeek (DLVO) theory to discard the importance of electrostatic interactions. We hypothesize then that the observed phenomenology is due to collective particle motions driven by gravity and mediated by hydrodynamic interactions that could yield formation of particle swirls driving them towards the unexpected plate. In fact, we find that the characteristic time for this process scales with height as do the magnitude of velocity fluctuations. Once these decay, particles do not move against gravity anymore. We emphasize that (i) our geometry differs from that of others, in that the container smaller dimension is along the direction of gravity, and that (ii) typical Péclet numbers in our experiments are of the order of 10^{-3}.

The rest of the paper is organized as follows. Section II describes the experiment. In Sec. III we describe the observed phenomenology, discuss the possibility of electrostatic adsorption, and describe the observations in terms of gravitationally driven particle motions. We then verify the crucial effect of gravity by performing an experiment with a density matched system; the phenomenon disappears. Finally we conclude in Sec. IV.

II. EXPERIMENTAL SYSTEM AND SETUP

The experimental cell is formed with two glass slides, coated with a chlorine terminated polydimethylsiloxane telomer (GlassClad 6C, FluoroChem, UK). The coating procedure consists in cleaning the original glass slides in an ethanol-acetone mixture, rinsing thoroughly with distilled water and immersing in a 3% solution of the coating in hexane for 20 min. After this last step, the slides are cured inside an oven for another 20 min at temperatures typically close to 100 °C; this enhances evaporation of any hexane rests and warranties a uniform coating throughout the slides, preventing irreversible sticking of the particles. The plates are separated by means of two poly(ethyleneterephthalate) spacers of constant height L_z varied between 23 and 1100 μm along the gravitational direction; these fix the cell height. We also employ (indium-tin-oxide)-coated glass slides (ITO, Delta Technologies LTD, USA) connected to ground, to check the influence of any electrostatic interactions between the confining walls and the colloidal particles.

The gap is filled with an electrostatically stabilized colloidal dispersion of sulphate-charged polystyrene particles provided by Ikerlat Polymers (Spain). The provided surface charge density and particle diameter, as determined by disc centrifuge, are $\sigma_s = 22.4\ \mu C/cm^2$ and $2a = (964 \pm 10)$ nm, respectively; the latter agrees with the size obtained by dynamic light scattering, $2a = (980 \pm 20)$ nm. Finally, the cell is sealed with bisphenol-A-epiclorhydrine epoxy glue. Particle volume fractions are always below $\phi = 10^{-3}$; above that value, sample opacity prevents observation with optical microscopy.

The surrounding solvent is a mixture of H_2O and D_2O to give a final density mismatch between the particles and the medium $\Delta\rho = \rho_{particle} - \rho_{medium}$. Low values of $\Delta\rho$ imply dynamics in the scale of hours to days, facilitating the observation of the phenomenology involved. The beginning of the experiment is set after sonicating the cell for 2 min to ensure the homogeneity of the initial state; the coating of the slides allows ultrasounds to resuspend particles adsorbed onto the walls.

The experimental setup depicted in Fig. 1 is mounted on the stage of an inverted microscope (Leica IM-DRB) and observed with a 40× (numerical aperture NA=0.55) objective lens giving a total magnification of 152 nm/pixel. The viewing area equals $117 \times 87\ \mu m^2$. Images are taken by means of a Sony DX-390P CCD camera mounted in the body of the microscope and captured by a CG-7 RGB Color Frame Grabber coupled to a PC.

III. RESULTS AND DISCUSSION

Snapshots for a typical experiment with $\Delta\rho = 4\ Kg/m^3$ and $\phi = 7 \times 10^{-4}$ are shown in Fig. 2. As expected, the number of particles N in the lower plate increases with time due to the particle-medium density mismatch, that leads to sedimentation [Figs. 2(a)–2(d)]. Surprisingly, N also increases in the upper plate [Figs. 2(e)–2(h)]. There are particles moving against gravity.

To quantify these visual observations we measure N as a function of time. To do so, we determine the particle centers and count them [21]. The number of particle counted images yielding a statistical meaningful N was determined from the percentage dispersion rate $T\%$ of three images. In most cases $8\% < T\% < 15\%$, implying that averaging over 15 images is enough [22]. The result for $\phi = 7 \times 10^{-4}$ and $L_z = 400\ \mu$m is presented in Fig. 3. We confirm that N increases with time in both upper and lower plates. We also see that for times larger than a characteristic time τ, N is constant. We define this time τ as the time at which the number of particles in either plate is 95% of the plateau value. Also visible is the stratification induced by gravity along its direction. The number of particles increases with decreasing height, as expected; this is fulfilled except for the particles at $L_z = 400\ \mu$m. We also note that at time $t=0$, the number of particles in the proximity of the planes is always smaller than that in the bulk indicating that the particles are excluded from the region close to the planes. With increasing t, the colloids overcome this repulsion and adsorb onto the plates; this adsorption is reversible due to the presence of the coating.

Changing the effective direction of gravity by setting $\Delta\rho \approx -10\ Kg/m^3$ does not alter the observed phenomenology. The particles now float or sediment upwards and as before, N increases in both lower [Figs. 4(a) and 4(b)] and

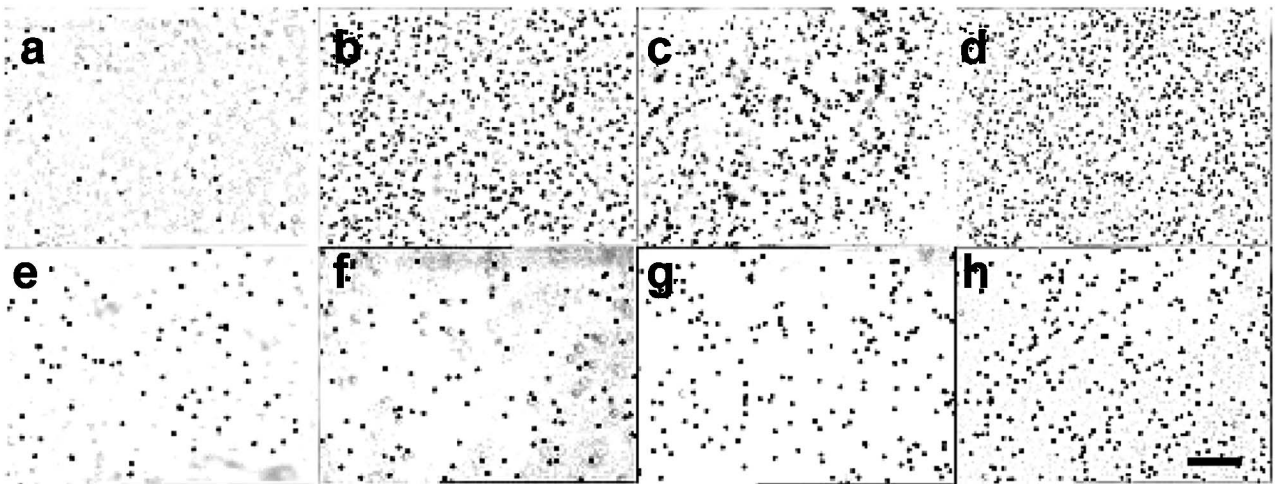

FIG. 2. Stages of evolution for both lower (a)–(d) and upper (e)–(h) plates for $\phi \approx 7 \times 10^{-4}$ and $L_z = 500$ μm. Snapshots were taken at $t=0$ h (a),(e); $t=8$ h (b),(f); $t=24$ h (c),(g); $t=48$ h (d),(h). As can be observed, there is an increasing number of particles at both plates with time. The scale bar corresponds to 20 μm.

upper [Figs. 4(c) and 4(d)] plates. Particle migration again occurs along and opposite to the gravitational direction.

It is well known that some surface silanol glass groups in the presence of water can dissociate to negatively charge the glass [23,24]. Even though this would not induce an attraction between the negatively charged particles and the glass, we performed experiments with grounded ITO-coated glass slides to check the influence of this effect. We found no appreciable differences with our previous observations. Additionally, we also used uncoated glass slides and uncoated ITO-covered plates to confine the suspensions without finding any significant differences with respect to the experiments reported. Our observations arise from the intrinsic behavior and properties of our system, and do not seem to be controlled by the characteristics of the confining surfaces.

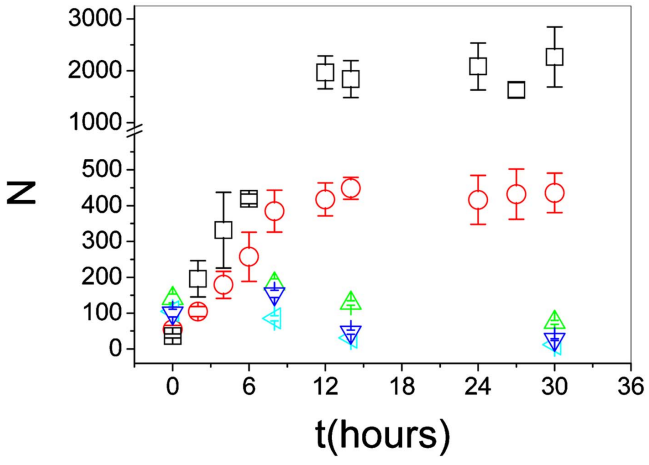

FIG. 3. (Color online) Quantitative evolution of the number of particles N with time for $\phi \approx 7 \times 10^{-4}$ and $L_z = 400$ μm. The particle-medium density mismatch is equal to $\Delta\rho = 4$ Kg/m^3. The symbols correspond to different heights: (□) $z=0$, (△) $z=100$ μm, (▽) $z=200$ μm, (◁) $z=300$ μm, (○) $z=400$ μm. The number of particles in both plates increases with increasing time until $t \approx \tau$. Above τ, N plateaus in the upper plate.

The observed phenomenology could arise from an electrostatically driven adsorption phenomenon [9], since the particles are charged. The migration of particles could then have its origin in their mutual electrostatic repulsion; the system evolves to an equilibrium state where particles accumulate onto the confining plates exclusively due to the electrostatic pressure exerted by the particles in the bulk. Driving particles to the boundaries then reduces the overall electrostatic energy of the system.

To test this possibility, we estimate the interaction between two particles a distance r apart with the repulsive part of the DLVO potential [25]: $U(r) = \frac{Q^2}{4\pi\varepsilon\varepsilon_0(1+\kappa a)^2}\frac{e^{-\kappa(r-2a)}}{r}$, substituting the particle bare charge Q for its effective charge Q_{eff}, as obtained with the aid of electrophoresis. In the previous equation, $\kappa = \sqrt{\frac{2e^2}{\varepsilon\varepsilon_o k_b T} N_A c}$ is the inverse of the Debye length, with e the electron charge, N_A the Avogadro number, k_B the

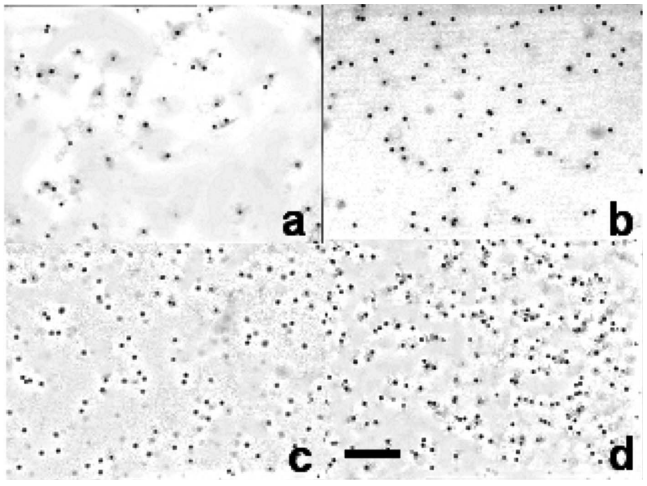

FIG. 4. Stages of evolution for both lower (a),(b) and upper (c),(d) plates for $\phi = 5 \times 10^{-4}$ and $\Delta\rho \approx -10$ kg/m^3. The effective gravitational direction points towards the upper plate. As can be observed, N increases from $t=0$ (a),(c) to $t=48$ h (b),(d). The scale bar corresponds to 20 μm.

Boltzmann constant, T the absolute temperature, c the salt concentration, ε the relative dielectric constant of the solvent, and ε_o the vacuum permittivity.

Electrophoretic mobility experiments can be used to estimate the particle effective charge. In such experiments an electric field E is applied and the particle velocity measured to yield the electrophoretic mobility μ. For small E fields: $v=\mu E$ [26]. The Smoluchowski Eq. [27] allows the proportionality coefficient μ to be related to the so called ζ potential, the electrostatic potential at the shear plane, in the limit $\kappa a \gg 1$. In this situation, the particle velocity is determined from the balance between electric and viscous forces, resulting in $\mu=\frac{\varepsilon\varepsilon_0}{\eta}\zeta$, where η is the solvent viscosity. In the high salt limit under consideration and assuming the small E fields do not distort the equilibrium configuration of the electric double layer, the ζ potential can be approximated by the surface potential in the absence of E:

$$\zeta = \psi\big|_{r=a}^{E=0}$$

with

$$\psi\Big|_{r=a}^{E=0} = \frac{Q_{eff}}{4\pi\,\varepsilon\varepsilon_o\,(1+\kappa a)a},$$

as obtained by solving the Debye-Hückel Eq. [28]. After substitution of this equation into the mobility expression, we obtain

$$\mu = \beta c^{-1/2}, \quad \beta = Q_{eff}\sqrt{\frac{\varepsilon\,\varepsilon_o k_b T}{32 N_A\,\pi^2 e^2 a^4 \eta^2}}. \tag{1}$$

Measurements of μ vs salt concentration allow Q_{eff} to be determined. The results of these experiments are presented in Fig. 5(a) [29,30]. As can be seen, we find that μ scales with salt concentration as $\mu \sim c^{-0.5}$, in agreement with Eq. (1). From the resultant linear fit of the data, we can extract a slope β, allowing Q_{eff} to be estimated. We obtain $Q_{eff}=(8\pm1)\times10^3 e$, a value that is approximately three orders of magnitude lower than the particle bare charge $\sigma_s 4\pi a^2 \approx (44\pm2)\times10^5 e$.

With this Q_{eff} estimate, we can determine the repulsion between particles. The result is plotted in Fig. 5(b). It is readily seen that particles separated by more than $r\approx4.1a$ interact with a strength below thermal energy k_bT. Considering that the mean interparticle distance is given by $\bar{d}=\left(\frac{V_p}{\phi}\right)^{1/3}$, with V_p the particle volume, we obtain $\bar{d}\approx16a$ for $\phi=10^{-3}$. Under these conditions, no electrostatically driven adsorption can occur; the electrostatic repulsion between particles cannot cause the observed particle migrations.

We then consider the other important force acting on our system; it arises from the fact that the particles are in the presence of the earth's gravitational field. This force together with buoyancy is responsible in most practical situations for sedimentation and creaming of colloidal suspensions. The velocity of an isolated sedimenting sphere is the well-known Stokes velocity:

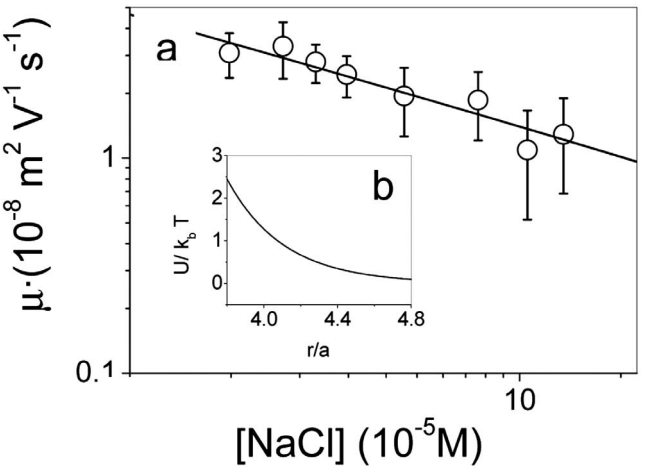

FIG. 5. (a) Electrophoretic mobility μ as a function of concentration c of a 1:1 electrolyte (NaCl). The condition $\kappa a\approx1$ is fulfilled for $c\approx2\times10^{-7}$ M and thus the experiments are performed in the high κa limit. In addition, $\phi=1.8\times10^{-5}$ and the experiment is performed under simple scattering conditions and in the absence of particle-particle interactions. As expected, μ decreases with c as $\mu\sim c^{-1/2}$. The solid line is the best least squares linear fit of μ vs $c^{-1/2}$. From the slope of this fit, we estimate the particle effective charge. (b) Particle-particle DLVO repulsive interaction potential for the experimental system under consideration. Note that for $r>4.1a$, $U<k_bT$ and electrostatic interactions between particles can be neglected at the experimental volume fractions.

$$v_s^0 = \frac{2}{9}\frac{\Delta\rho g a^2}{\eta} \tag{2}$$

with g the acceleration of gravity. A uniform concentration of particles falls more slowly because of the backflow arising from confinement [31]:

$$v_s = v_s^0(1-6.55\phi+\Theta[\phi^2]). \tag{3}$$

Additionally, fluctuations $\delta v=v-v_s$ about the mean velocity of the colloidal particles, which are driven by long-range interparticle hydrodynamic interactions, appear during the sedimentation process [12–20]. These fluctuations decay exponentially with time:

$$\delta v = \delta v_0 e^{-t/\tau_s}, \tag{4}$$

where δv_0 is the initial value of the fluctuations and τ_s is a relaxation time related mainly to the spreading of the sedimentation front [18,20]. This relaxation time is only dependent on the container height and scales with it as $\tau_s \sim L_z^{1.2}$ [18].

We explore the influence of L_z in our system and obtain that the characteristic time for N to plateau increases with plate-to-plate separation (Fig. 6). Moreover, τ depends on L_z as $\tau\sim\left(\frac{L_z}{2a}\right)^{1.20\pm0.05}$ for almost two decades. To ensure that the slope reported is only due to changes in plate separation, all the experiments were performed for the same volume fraction $\phi\approx7\times10^{-4}$ and density mismatch $\Delta\rho\approx4$ Kg/m^3. The encountered scaling law quantitatively agrees with that found by Shang *et al.* [18] for the characteristic decay time of velocity fluctuations. It thus seems that our results are reminis-

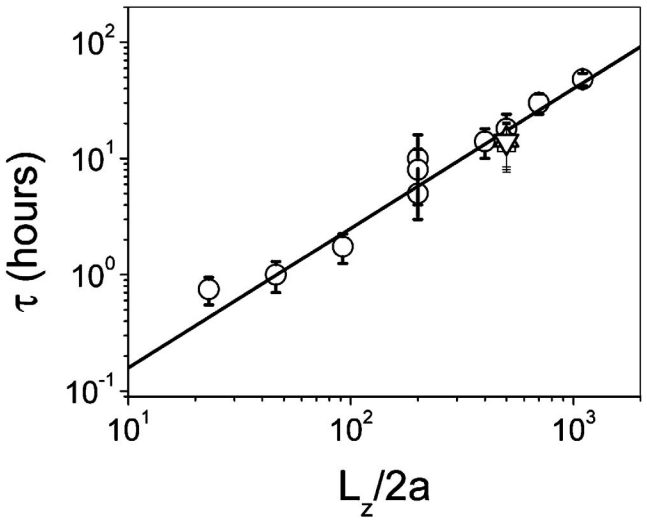

FIG. 6. Characteristic time τ as a function of a normalized plate-to-plate separation distance. Different symbols represent experiments with different types of confining plates: (○) glass coated with GlassClad; (□) glass coated with ITO; (△) glass coated with ITO and GlassClad; (▽) plain glass. Plates coated with ITO are connected to ground to assure wall charge is zero. The solid line represents the best fit to the data in a log-log scale. We obtain $\tau \sim \left(\frac{L_z}{2a}\right)^{1.20\pm0.05}$.

cent of those of Shang *et al.* and that the increase of N in the upper plate (lower plate in the case of $\Delta\rho<0$) is related to sedimentation induced swirls that drive the particles against the gravitational direction. The characteristic time τ of our experiments could then be interpreted as the time it takes for velocity correlations to sufficiently decay [32]. Considering an intermediate height value of $L_z=400$ μm, we can estimate the ratio of velocity fluctuations to the mean sedimentation velocity as $\frac{\delta v_0}{v_s} \sim \left(\frac{L_z}{2a}\right)^{2/3}\phi^{1/3}$ [12] to be $\frac{\delta v_0}{v_s} \approx 1$, thus confirming that these are indeed relevant in our experimental conditions. We can also estimate the maximum swirl dimension as $l \sim a\left(\frac{L_z}{2a}\right)^{2/3}\phi^{-1/3}$ [18] to get $l \approx 300$ μm. This value is reasonable and implies that particles as much as 300 μm far away from the upper plate might eventually move towards the plate in a collective swirl and against the direction of gravity. This estimate of l is the upper bound value for a swirl dimension; most likely the swirl size will be smaller [12].

Despite the agreement between our results and those of Shang *et al.* [18], there are important differences we would like to emphasize. One of them concerns the geometry. In our experiments, the smallest dimension lies within the direction of gravity and is not perpendicular to it, as in most sedimentation experiments. This could in principle influence swirl formation if the time scale associated with sedimentation is smaller than that needed to form a swirl; this would then prevent particles from rising up when $\Delta\rho>0$. Our results, however, seem to indicate that swirls have time to develop and that some particles are indeed driven to the upper plate (bottom plate when $\Delta\rho<0$). In addition, we see that N plateaus. This implies that particles bind to the walls once they get there [33]. In the absence of this binding, N would rise, reach a maximum, and then decrease. The maximum would then reflect the characteristic time τ that we have measured. Finally, Péclet numbers in our experiments are well below 1, in contrast to the experiments of Shang *et al.* [18]; this emphasizes the Brownian character of our experimental system at short time scales. However, at longer times the system is dominated by sedimentation with particle migrations resembling those typically seen in non-Brownian systems.

The mixed diffusion and settling motions of our particles should give rise to a steady state density profile characterized by the gravitational length l_g. In this steady state, the flux of particles induced by sedimentation must balance an opposite flux due to diffusion of particles along the particle number concentration n gradient:

$$D\frac{dn}{dz} = nv_s. \tag{5}$$

The steady state particle concentration profile is readily obtained after integration and use of Eq. (2) for v_s and the Stokes-Einstein expression for D [34]:

$$n(z) = n_0 \exp(-z/l_g), \tag{6}$$

where $n_0=n(z=0)$ and $l_g=\frac{k_bT}{\Delta\rho V_p g}$.

To obtain a gravitational length from the experiments, we must recognize that $n_o=n_o(L_z)$. The link between these can be obtained by integrating Eq. (6) over the sample volume to obtain the total number of particles:

$$\int_0^{L_Z} n(z)dz = \frac{\phi L_z}{V_p}. \tag{7}$$

In order to obtain a single l_g using data for different cell heights, this dependence must be accounted for. We thus decided to follow an iterative process to obtain both l_g and $n_o(L_z)$. An initial l_g^0 is used to calculate n_o^0 for the different L_z values through Eq. (7). We then perform a linear fit of $\ln(n_o^0/n)$ vs z yielding a second value for the gravitational length l_g^1, that we use to calculate a new value of $n_o(L_z)$, namely n_0^1. The process is repeated until $|l_g^n - l_g^{n-1}| < 10^{-8}$. Finally, we check that the final l_g^n is independent of the first seed. For all seeds tested, the iteration converges in less than 20 steps.

The final experimental steady state sedimentation profiles are presented in Fig. 7. The plot includes different L_z and as can be seen the data collapse onto a single curve, as expected after taking the $n_o=n_o(L_z)$ dependence into account. From the slope of the final linear fit we obtain a gravitational length of $l_g=(16\pm6)\times10$ μm, that is in reasonable agreement with the theoretical value $l_g=224$ μm. Data corresponding to the top and bottom plates have not been included in the graph due to particle-wall interactions. Perhaps this effect is responsible for the large scatter in the data as reflected by the large l_g error.

As a final check to the key role played by gravity in our results, we perform an additional experiment with an almost perfect density matched system; the estimated density difference being less than 0.1 kg/m^3. The experimental conditions are $\phi \approx 10^{-3}$ and $L_z=200$ μm. Results are presented in Fig.

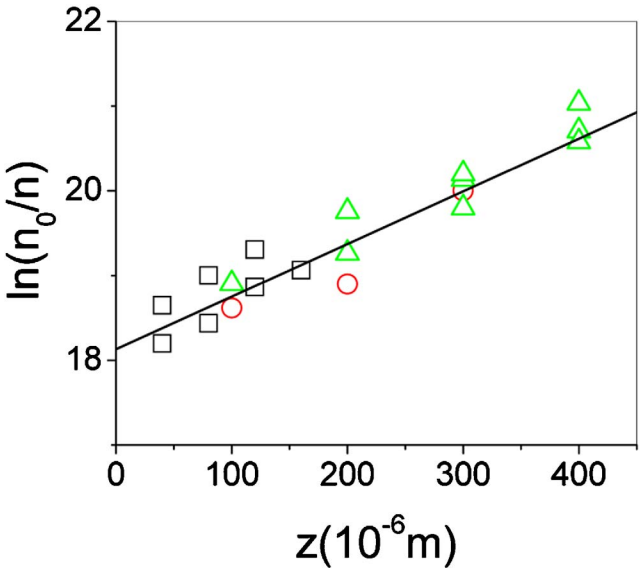

FIG. 7. (Color online) Experimental steady state sedimentation profile: $\ln(n_0/n)$ vs z. The symbols correspond to (□) $L_z=200$ μm, (○) $L_z=400$ μm, and (△) $L_z=500$ μm. The line is the best linear fit. The slope allows determination of the gravitational length.

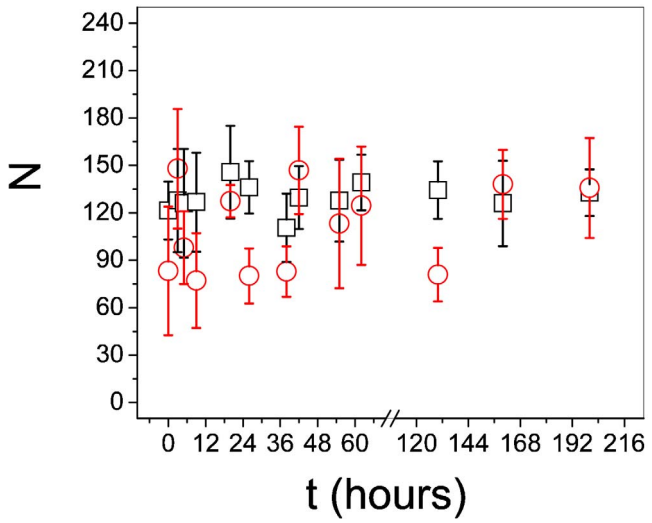

FIG. 8. (Color online) Number of particles N near upper (○) and lower (□) plates for $\phi \approx 10^{-3}$ and $L_z=200$ μm. The sample is density matched to approximately $\Delta\rho=0.1$ Kg/m^3. N is constant for the experimental time window (a week and a half), implying there are no particle migrations in this time frame.

8. No appreciable change in N is observed at any height; thus N does not increase in the upper or lower plates, at least within the experimental time window probed. This result emphasizes the crucial role played by gravity in the reported phenomenology. In addition, this result emphasizes the presence of a weak repulsive barrier between the particles and the plates, that is responsible for the lack of particle adsorption in this experiment and for the smaller number of particles near the plates at $t=0$, in the previously reported ones. Without the presence of this barrier, particles will increasingly stick to the confining walls due to diffusion; this would result in the adsorption of all particles onto the planes. The absence of a large enough buoyant particle mass and of sedimentation swirls allows this barrier to effectively prevent particle adsorption [36].

Finally we would like to remark on the appreciable variance of N in this final experiment. In view of the time scale involved, ambient temperature variations could modify the particle-medium density difference introducing the observed noise in N. We estimate that for temperature variations of ± 2 °C, the density difference $\Delta\rho$ could change in ± 0.4 Kg/m^3. Whereas these slight density changes could affect the experiment presented in Fig. 8, they are unlikely to play any significant role in all other experiments. In addition, we would like to emphasize that all samples were kept at room temperature throughout the length of the experiments and were only illuminated for image acquisition; this discards the presence of any temperature gradients that could induce sample convection.

IV. CONCLUSIONS

We have presented experiments of settling hard charged spheres in cells whose smallest dimension lies along the direction of gravity and found that the number of particles N near both upper and lower confining plates increases with time. The process occurs in a characteristic time τ, above which N plateaus. Estimates of the particles' effective charge via electrophoretic mobility experiments allows determination of the electrostatic repulsion between particles. The results rule out the electrostatically driven adsorption of particles onto the confining walls for the typical volume fractions of our experiments. The characteristic time of our observations scales with plate-to-plate separation as $\tau \sim L_z^{1,2}$; an identical scaling to that expressing the decay of particle velocity fluctuations in sedimentation processes. We thus tentatively conclude that particle migration occurs in our experiment due to velocity correlations mediated by hydrodynamic interactions; these induce formation of swirls that could drive the particles to the upper plate despite the system is sedimenting down. Our results support that these effects could be important irrespective on whether (i) the smallest cell dimension lies along or perpendicular to the direction of gravity and (ii) the Péclet numbers involved are as low as 10^{-3}.

ACKNOWLEDGMENTS

We acknowledge Ministerio de Ciencia y Tecnologia (Grant No. MAT2004-03581). We thank Phillip Morris USA for financial support. INEST Group is sponsored by PMUSA. We thank Shang-You Tee and Magdaleno Medina-Noyola for carefully reading the manuscript and Phil Segre for additional stimulating comments and discussions.

[1] Y. Levin, Rep. Prog. Phys. **65**, 1577 (2002).
[2] L. Bocquet, E. Trizac, and M. Aubouy, J. Chem. Phys. **117**, 8138 (2002).
[3] R. Messina, C. Holm, and K. Kremer, Phys. Rev. Lett. **85**, 872 (2000).
[4] V. A. Bloomfield, Biopolymers **31**, 1471 (1991).
[5] R. Podgornik, D. Rau, and V. A. Parsegian, Biophys. J. **66**, 962 (1994).
[6] A. V. Kabanov and V. A. Kabanov, Adv. Drug Delivery Rev. **30**, 49 (1998); Bioconjugate Chem. **6**, 7 (1995).
[7] S. Croll, Prog. Org. Coat. **44**, 131 (2002).
[8] D. J. Clements and E. Dickinson, *Advances in Food Colloids* (Blackie Academic & Professional, London, New York, 1995).
[9] P. Gonzalez-Mozuelos and M. Medina-Noyola, J. Chem. Phys. **93**, 2109 (1990); **94**, 1480 (1991); P. Gonzalez-Mozuelos, J. Alejandre, and M. Medina-Noyola, *ibid.* **95**, 8337 (1991); **97**, 8712 (1992).
[10] S. Ramaswamy, Adv. Phys. **50**, 297 (2001).
[11] E. S. Asmolov, Phys. Fluids **16**, 3086 (2004).
[12] M. P. Brenner, Phys. Fluids **11**, 754 (1999).
[13] A. J. C. Ladd, J. Fluid Mech. **271**, 285 (1994); Phys. Fluids **9**, 491 (1997); N. Q. Nguyen and A. J. C. Ladd, J. Fluid Mech. **525**, 73 (2005).
[14] E. Kuusela, J. M. Lahtinen, and T. Ala-Nissila, Phys. Rev. E **69**, 066310 (2004).
[15] P. Tong and B. J. Ackerson, Phys. Rev. E **58**, R6931 (1998).
[16] P. N. Segrè, E. Herbolzheimer, and P. M. Chaikin, Phys. Rev. Lett. **79**, 2574 (1997).
[17] P. N. Segrè, F. Liu, P. Umbanhowar, and D. A. Weitz, Nature (London) **409**, 594 (2001).
[18] S. Y. Tee, P. J. Mucha, L. Cipelletti, S. Manley, M. P. Brenner, P. N. Segre, and D. A. Weitz, Phys. Rev. Lett. **89**, 054501 (2002).
[19] H. Nicolai, B. Herrhaft, E. J. Hinch, L. Ogers, and E. Guazzelli, Phys. Fluids **7**, 12 (1995).
[20] P. J. Mucha, S. Y. Tee, D. A. Weitz, B. I. Shraiman, and M. P. Brenner, J. Fluid Mech. **501**, 71 (2004).
[21] J. C. Crocker and D. G. Grier, J. Colloid Interface Sci. **179**, 298 (1996).
[22] J. R. Taylor, *An Introduction to Error Analysis. The Study of Uncertainties in Physical Measurements* (University Science Books, Sausalito, CA, 1997).
[23] S. H. Behrens and D. G. Grier, J. Chem. Phys. **115**, 6716 (2001).
[24] R. K. Ilier, *The Chemistry of Silica* (Wiley, New York, 1972).
[25] B. V. Derjaguin and L. Landau, Acta Physicochim. URSS **14**, 633 (1941); E. J. Verwey and J. T. G. Overbeek, *Theory of the Stability of Lyophobic Colloids* (Elsevier, Amsterdam, 1948).
[26] R. J. Hunter, *Zeta Potential in Colloid Sciences* (Academic, New York, 1989).
[27] M. von Smoluchowski, Z. Phys. Chem., Stoechiom. Verwandtschaftsl. **92**, 129 (1917).
[28] R. J. Hunter, *Foundations of Colloid Science* (Oxford University Press, Oxford, 1986).
[29] The electrophoretic mobility measurements are performed with a ZetaSizer-Z (Malvern Instruments, UK). The measuring technique rests on classical Doppler electrophoresis [26], consisting in analyzing the mixing of scattered light from the colloidal suspension and a reference beam of well-known frequency in terms of the phase shift between the reference and the scattering beam in the so-called phase analysis light scattering [35]. From the rate of change of this phase difference, the velocity and therefore the electrophoretic mobility can be obtained.
[30] Prior to the electrophoretic mobility measurements of Fig. 5(a), we optimized particle volume fraction to assure simple-scattering conditions. We measured the scattering intensity I as a function of ϕ and obtained that above $\phi > 2 \times 10^{-5}$ the linear $I-\phi$ dependence disappears as a result of multiple scattering. The measurements are thus performed at $\phi = 1.8 \times 10^{-5}$.
[31] G. K. Batchelor, J. Fluid Mech. **52**, 245 (1972).
[32] If the encountered particle migrations were driven by diffusive processes, the characteristic time would scale with cell height as L_z^2, which is clearly different from our results. We note, however, that this L_z^2 dependence is, in principle, strictly valid in the absence of particle-wall interactions.
[33] We have assessed that there are particle-wall interactions by turning upside down the cell after a typical experiment and realizing that N did not change in the plate located in the bottom to begin with. Similar results were obtained irrespective of whether the glass slides were coated or not with ITO. This interaction is weak since sonication is able to remove all particles from the plates. If the GlassClad coating is not used, the binding is irreversible and the particles are not removed by sonication.
[34] R. Piazza, T. Bellini, and V. Degiorgio, Phys. Rev. Lett. **71**, 4267 (1993).
[35] J. F. Miller, K. Schäetzel, and B. Vincent, J. Colloid Interface Sci. **143**, 532 (1991); F. McNeill-Watson, W. Tscharnuter, and J. Miller, Colloids Surf., A **140**, 53 (1998).
[36] The nature of this barrier is uncertain. While it could arise from the detailed interaction between the plates and the particles, experiments with different plate surfaces yield the same results indicating that this is unlikely a plate dependent repulsion. Our results indicate that the height of this barrier, whatever its detailed origin, is enough to prevent particle adsorption in the "absence" of gravity. When the particles' buoyant mass is large enough, the barrier is overcome and the particles reversibly adsorb onto the plates.